Heliyon 10 (2024) e25963

Contents lists available at ScienceDirect

Heliyon

journal homepage: www.cell.com/heliyon

Research article

Preparation and characterization of polyvinyl alcohol (PVA)-glycerol composite films incorporating nanosilica from municipal solid waste incinerator bottom ash

Phan Thi Hong Hanh [a], Thitipone Suwunwong [b,c], Suchada Chantrapromma [d], Patcharanan Choto [b,c], Chuleeporn Thanomsilp [b], Khamphe Phoungthong [a,e,*]

[a] Faculty of Environmental Management, Prince of Songkla University, Songkhla, 90112, Thailand
[b] School of Science, Mae Fah Luang University, Chiang Rai, 57100, Thailand
[c] Center of Chemical Innovation for Sustainability (CIS), Mae Fah Luang University, Chiang Rai, 57100, Thailand
[d] Division of Physical Science, Faculty of Science, Prince of Songkla University, Songkhla, 90112, Thailand
[e] Hub of Waste Management for Sustainable Development, Center of Excellence on Hazardous Substance Management, Chulalongkorn University, Bangkok, 10330, Thailand

ARTICLE INFO

Keywords:
Solid waste
Nano SiO_2
Polyvinyl alcohol
Sol-gel method
Nanocomposite wrapping films

ABSTRACT

This study investigates the fabrication of a composite film composed of polyvinyl alcohol (PVA) and glycerol, incorporating nanosilica derived from municipal solid waste incinerator bottom ash (BA). The nanosilica is blended with a PVA film-forming solution containing glycerol as a plasticizer. The composite films are characterized using Fourier transform infrared spectroscopy (FTIR), X-ray diffraction (XRD), and scanning electron microscopy (SEM). Additionally, thermogravimetric analysis (TGA) is conducted to evaluate the thermal properties, while the mechanical properties are assessed in terms of tensile strength (TS) and elongation at break (EAB). The results indicate that the presence of silica nanoparticles reduces transparency and increases film thickness in the presence of glycerol. Notably, the film containing 1% silica demonstrates a significant enhancement in tensile strength, exhibiting a 50% increase compared to the film without silica. However, higher silica loadings lead to a deterioration in mechanical properties due to silica agglomeration within the polymer matrix. As expected, the presence of silica in the films slightly elevates the degradation temperature.

1. Introduction

Nowadays, there is growing concern over the environmental sustainability issue due to the overuse of plastic packaging film, which has impelled the advancement of biopolymer research [1]. As a result, bioplastics have drawn a lot of interest as a sustainable option for packaging applications [2]. Polyvinyl alcohol (PVA), a biopolymer, is recognized as a promising replacement for petrochemical-derived plastics, particularly in packaging contexts. PVA exhibits elevated hydrophilicity, robust compound stability, and remarkable film-forming characteristics, rendering it endowed with a plethora of advantageous attributes for deployment in packaging film [3–5]. However, PVA has some limitations including low thermal stability, and high moisture absorption when used in

* Corresponding author. Faculty of Environmental Management, Prince of Songkla University, Songkhla, 90112, Thailand.
E-mail addresses: honghanh.phan.env@gmail.com (P.T.H. Hanh), thitipone.suw@mfu.ac.th (T. Suwunwong), suchada.c@psu.ac.th (S. Chantrapromma), patcharanan.cho@mfu.ac.th (P. Choto), chuleeporn@mfu.ac.th (C. Thanomsilp), khamphe.p@psu.ac.th (K. Phoungthong).

https://doi.org/10.1016/j.heliyon.2024.e25963
Received 5 September 2023; Received in revised form 30 November 2023; Accepted 5 February 2024
Available online 7 February 2024

packaging [6]. The hydrogen bonding groups included in the PVA structure make it easier to combine nanocomposites with other organic and inorganic nanomaterials to enhance these properties and enrich the functionality of the polymer [7,8]. Moreover, many studies have been working to enhance the physicochemical and structural properties of the polymer, and they are particularly concerned with how the chain structure, crystallization, density, chain orientation, and packing state of polymer materials affect its penetration behaviors [9,10], the interaction between molecular size, framework, and polarity of the penetration and the material structure, which affects permeation behaviors [11,12] and the influence of polymer laminar blending on permeation behaviors [13, 14]. Also, they create a variety of barrier materials and enhance the barrier qualities of materials using blocking technologies, including surface treatment [15], blends [16], nanocomposites [17], etc. In the investigation conducted by Liu et al., in 2008, they examined the PVA/titanium dioxide nanocomposite. Their findings indicated that as the concentration of carboxylated nano-TiO_2 increased, there was a notable reduction in the loss tangent and a substantial enhancement in the storage modulus. These effects led to a significant improvement in the tensile strength of the nanocomposites [18]. Nagalakshmi et al. (2010) proved that the thermal stability of PVA/NiO nanocomposites was enhanced with increasing NiO amount [19]. ZnO–SiO_2 nanocomposites were infused into PVA/CS film to enhance the shelf life of food products [20]. Salman et al. (2018) proved the capacity of PVA/nanocellulose/Ag nanocomposite films with excellent mechanical and microbiological properties, and this film can be used as antimicrobial food packaging materials [21]. Abdullah et al. (2019) prepared transparent and biodegradable water-resistant poly(vinyl alcohol)/-starch/glycerol/halloysite nanotube nanocomposite films for sustainable food packaging of lipophilic and acidic foodstuffs [22]. Moreira et al. (2020) developed an edible antimicrobial covering made of polysaccharide/PVA which is bio-active and environmentally friendly. It reduces water loss from fresh fruit storage and prevents the growth of fungi [23]. Their studies reported that composites created by combining different nanomaterials had better functional properties than pure PVA.

Among the variety of nanoparticles, silica has numerous characteristics including their biocompatibility and biodegradability, large surface areas, and abundant numbers of silanol groups. These attributes collectively contribute to the establishment of a more robust interface with polymers in composite materials, boost the efficacy of hydrogen bonding interaction and induce modifications in the crystalline behaviors within the polymeric matrix blend [24]. Therefore, in recent years, SiO_2 has also been frequently employed to modify polymeric materials due to its nontoxic, affordable, strong barrier, and high mechanical qualities [20,25]. SiO_2 has been proven to be an excellent nucleating agent for crystallization and thermal stability as well as for increasing the strength and barrier of polymers, thereby improving the general performance of composites [3,26]. Nevertheless, tetraethyl orthosilicate (TEOS) as the silica source is quite pricey. Therefore, SiO_2 derived from renewable resources has been the center of public concern for environmental conservation and sustainable development.

The main components of Municipal Solid Waste Incineration (MSWI) Plant ashes consist of a large amount of SiO_2, therefore, it is a kind of silica source with a cheap price. Generally, utilization of the waste residues from incineration and combustion plants for production of silica-based materials is indeed viable. Several research endeavors have demonstrated success in repurposing such residues, notably through processes like the conversation of residue into zeolite via alkali-based methods [27], the synthesis of zeolitic material, and the extraction of SiO_2 from MSWI ash [28]. Furthermore, in a noteworthy milestone achieved in 2007, the successful synthesis of mesoporous silica materials, including MCM-41, SBA-15, and SBA-16, was accomplished using power plant bottom ash as a precursor [29]. Additionally, mesoporous silica has been prepared through a sol-gel approach employing municipal solid incineration bottom ash [30], and industrial fly ash [31]. Silica nanoparticles were synthesized from sugar industry bottom ash [32], and paper industry fly ash [33] with an alkaline extraction method. This study aims to investigate the production of silica nanoparticles through the alkaline extraction method using Bottom Ash (BA) from MSWI. The extracted SiO_2 nanoparticles are then incorporated into a composite film consisting of PVA and glycerol.

To our knowledge, the characteristic of PVA/glycerol film containing SiO_2 nanocomposite films has been less reported. Therefore, this study aimed to improve PVA packaging by incorporating nano-SiO_2 through the sol-gel process, utilizing glycerol as a plasticizer, to develop novel biodegradable films for packaging applications. The investigation focused on assessing the impact of SiO_2 concentration in the composite films on the structural properties, and mechanical, thermal, and optical characteristics of the resulting PVA/glycerol films containing SiO_2.

2. Materials and methodologies

2.1. Materials

In this study, silica was extracted from the Bottom Ash (BA) which was obtained from Municipal Solid Waste Incineration Plant located at Saphan Hin, Phuket, Thailand. Poly(vinyl alcohol) was purchased from Sigma-Aldrich, Saint Louis, USA; Hydrochloric Acid (HCl) 37%; Glycerol ($C_3H_8O_3$) was brought from Qrec, Newzealand; Sodium hydroxide (NaOH) 98%, Loba Chemie PVT.LTD, India.

2.2. Methodologies

2.2.1. Extraction of silica from bottom Ash-Municipal Solid Waste Incineration Plant

Firstly, the ingredient of BA material was examined by the X-ray Fluorescence (XRF, S2175 Ranger, Bruker, Burladingen, Germany) analysis before doing experiments, and the result was listed in Table S1.

The (BA)-municipal solid waste incineration which includes 37.5% SiO_2 content as the main component (Table S1 in the Supplementary material) was used as raw material for extraction of SiO_2. The large granular ash was ground into small particles using a ball-mill grinder for 5 min. The resulting particles with a size less than 1 μm were collected using a mesh, and were used for silica

Table 1
The film compositions.

Formulation	Glycerol (wt.%)	Silica (wt.%)
PVA-Si 0	10%	0
PVA-Si 0.5	10%	0.5%
PVA-Si 1	10%	1%
PVA-Si 3	10%	3%
PVA-Si 5	10%	5%
PVA-Si 7	10%	7%

wt.% of dry PVA.

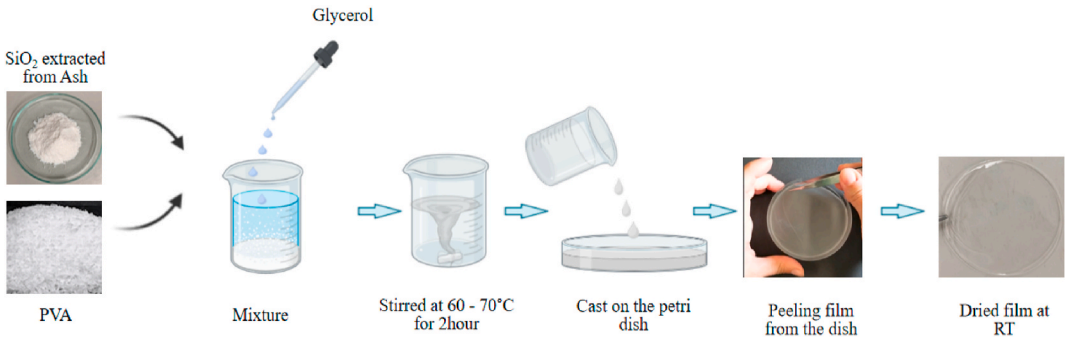

Fig. 1. The diagram making the composite SiO_2/PVA-Glycerol film.

extraction with an alkaline method. The fine powder was then washed multiple times with distilled water, and dried in an oven at 90 °C for one day.

In the round bottom flask, 5 g BA powder was stirred with 100 mL of 4 M NaOH solution, and then refluxed at 90 °C, for 16 h. The reaction solution was then filtered through a 0.45 μm membrane, and the filtrate was collected for adjusting pH at 7 by using HCl 5 M and continued aging at room temperature for 24 h. The precipitated product was washed several times with hot distilled water and dried at 80 °C for 24 h. The collected silica was analyzed again with X-ray Fluorescence (XRF, S2175 Ranger, Bruker, Burladingen, Germany) to check for impurities of Silica (SiO_2 accounted for 83%), which is shown in Table S2.

2.2.2. Film preparation

To prepare PVA films added with Silica, 1 g PVA pellets were dispersed in 10 mL distilled water. Glycerol was employed as a plasticizing agent, and Silica powder was added into the mixture. The varied amounts of silica as the weight percentage of dry PVA are shown in Table 1. Then the mixture was stirred continually at 60–70 °C until achieve the homogeneous solution. The PVA solution was cast on the polystyrene petri dish and dried at 25 °C for 24h. Finally, the films were detached from the petri dish. A comparison was made between the pure PVA film, devoid of silica, and the films containing silica. The step-by-step making of the composites SiO_2/PVA-Glycerol film is shown in Fig. 1.

2.3. Film characterization

2.3.1. Film thickness and opacity

A digital micrometer (Model) was used to measure the thickness of the film at 5 random positions of each film.

The method was used to measure the opacity of films by cutting the film into a strip (10 mm × 40 mm) and putting it along the inside wall of a cuvette. The UV–Vis spectrophotometer at 600 nm (A600) measured the absorbance. Another empty cuvette was used as a reference standard. The opacity of film (O) was determined using the following formula (E1) [34,35].

$$O = \frac{A_{600}}{t} \quad \text{(E1)}$$

where.

- t is the film's thickness (mm).
- The absorbance value at 600 nm is A600.

2.3.2. Fourier transform infrared (FTIR) spectroscopy analysis

All films and Silica nanoparticles were analyzed with an FTIR spectrophotometer (Thermo Fisher, Nicolet iS5, USA). The sample was measured in wavelengths of 4000 to 400 cm^{-1}.

Table 2
The thickness, and opacity of the composite film.

Film sample	Thickness (mm)	Opacity (Abs600/nm)
PVA-Si 0	15.02 ± 0.01	0.44 ± 0.07
PVA-Si 0.5	15.20 ± 0.01	0.49 ± 0.04
PVA-Si 1	14.98 ± 0.04	0.50 ± 0.02
PVA-Si 3	14.97 ± 0.02	0.52 ± 0.41
PVA-Si 5	14.99 ± 0.03	0.53 ± 0.04
PVA-Si 7	15.07 ± 0.01	0.96 ± 0.22

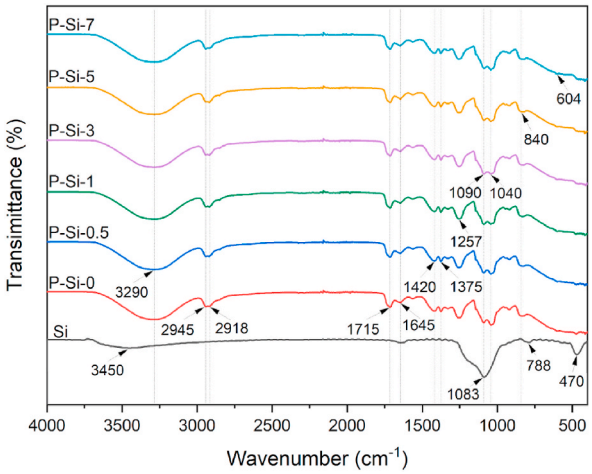

Fig. 2. FTIR of PVA/glycerol films combined with silica nanoparticles.

2.3.3. X-ray diffraction (XRD) analysis

The XRD was performed on an X'Pert PRO X-ray diffractometer (X'Pert Pro MPD, Malvern Pananalytical, Bruker AXS Advance, United Kingdom) with a CuKα radiation source (40 kV, 40 mA, and λ = 0.15406 nm) in the wide-angle X-ray diffractometer (WAXD) patterns. The data were captured at a scanning speed of 8°/min, in the 2θ range from 5° to 60°, with a scale factor of 0.02°.

2.3.4. Scanning electron microscope (SEM)

In a high vacuum and at an accelerating voltage of 12–15 kV, an SEM (Apreo, FEI, South Moravian Region, Czech Republic) was used to examine the surface and cross-section morphologies of the film. Before observation, the films were coated with gold and affixed to the specimen holder using conductive glue. Magnifications ranging from 500 to 3000x were used to visualize.

2.3.5. Mechanical properties

According to ASTM standard method D882-09, (Standard, 2009), tensile strength (TS) and elongation at break (EAB%) were measured at room temperature (25 °C) by using an INSTRON 5566 Machine with a tensile rate of 5 mm/min and 10 kN of tensile load. The films were conditioned in the desiccator for at least 2 days before testing. The films were cut into 100 mm × 500 mm strips and then measured at least five times for each sample, and the average of the results was calculated. Values tensile strength (TS) and elongation at break (EAB) were derived from the Instron Bluehill Universal Software (Norwood, MA, USA).

2.3.6. Thermal characterization

- Thermogravimetric analysis (TGA)

Firstly, the samples of film weighed between 7 and 10 mg and were placed in the thermal analyzer (TGA/DSC 3+, Mettler Toledo, Switzerland), which ran from 30 °C to 700 °C. Under a nitrogen environment, the TGA was conducted at a heating rate of 10 °C/min.

3. Results and discussion

3.1. Film thickness and opacity

Thickness serves as a crucial indicator for evaluating the functional properties of the film. The data reported in Table 2 showed that the thickness value slightly increased when adding more silica content. This might be caused by the CH-based film-forming solution's

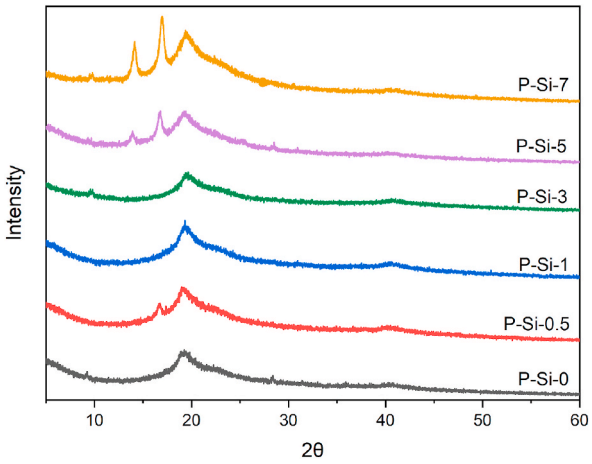

Fig. 3. XRD patterns of film combined silica nanoparticles and PVA/glycerol.

increased viscosity [36], leading to an impact on the resulting materials' thickness [37].

Because the appearance of the packaging film has a significant impact on customer desirability, the opacity of the materials was assessed by measuring the light transmission through the films at a wavelength of 600 nm.

Table 2 demonstrates that the opacity of the films increased with higher silica content. The visual observation of the specimens, as depicted in the imagery, corresponded congruently with the outcomes derived from the film opacity measurements. This alignment suggested that the presence of silica had a light-inhibiting effect on the film, resulting in reduced light transmission. The observed reduction in light transmission can be attributed, at least in part, to the light-scattering phenomenon.

3.2. FTIR spectroscopy analysis

FTIR spectra were used to identify the presence of certain functional groups in the molecular structure of the composites. Fig. 2 illustrates the FTIR spectra of PVA/Glycerol films and blending with the different percentage silica nanoparticles. For all films tested, their spectra showed –OH stretching between 3500 cm^{-1} and 3100 cm^{-1}, –CH2- asymmetric stretching, and symmetrical bending at 1945 cm^{-1}, 2918 cm^{-1}, 1420 cm^{-1}, 1357 cm^{-1} [38]. The peak located at around 1040 -1090 cm^{-1} in all spectra might be associated with glycerol [38]. The stretching of C═O and C–O from acetate groups remaining in partially hydrolyzed PVA was viewed at the peak of around 1715 cm^{-1} [39]. Additionally, the strong bands at 1083 cm^{-1}, 788 $cm^{-1,}$ and 470 cm^{-1} were associated with the asymmetric, and symmetric Si–O–Si stretching vibration bonding [40]. The appearance of a wider peak at around 1040–1090 cm^{-1} in the Si–O–Si peaks also be indicative of the formation of a novel Si–O–C bond, denoting the creation of a Si–O–C linkage within the composite films through the cross-linking of silica and PVA [41].

3.3. XRD analysis

As shown in Fig. 3, all films' diffraction peaks could be seen at 2 theta = 19.3°, indicating PVA's semi-crystalline phase [3,21,38,42]. As the amount of silica in the sample increased, the strength of the peaks at 2theta = 19.3° was slightly broader, showing that the crystalline structure of the PVA films was a little weaker. These results matched up with the mechanical tests. Even though the crystallinity drop was slight, it demonstrated that the amount of SiO_2 added could have an impact on the PVA/glycerol films' crystallinity. Therefore, we can simply alter the mechanical characteristics of the PVA/glycerol biodegradable film by adjusting the SiO_2 content. The absence of silica's distinctive peaks in the films further suggested that silica was evenly distributed throughout the PVA matrix as a whole [40].

3.4. Film structure

The SEM micrographs in Fig. 4 depicted the PVA-Si composite films. Initially, the PVA-glycerol film without silica exhibited a uniform, and homogeneous surface and cross-section, as seen in Fig. 4a and A. However, as the silica content increased in the films (Fig. 4b–f), both the surface and cross-section became coarser and displayed signs of discontinuity. Furthermore, the inclusion of silica in the PVA film led to the appearance of small white spots, which became more concentrated with higher silica content. Notably, as the silica content increased from 0 to 3%, the silica particles were observed to be uniformly dispersed within the films. Nevertheless, in the PVA films containing 5% and 7% silica, some areas displayed aggregations of silica. These findings align with previous research indicating similar outcomes when SiO_2 was added to PVA films beyond a certain threshold [43]. These figures serve as clear evidence that the addition of silica nanoparticles to the PVA/glycerol film resulted in a nearly uniform surface without cracks, suggesting good compatibility between silica nanoparticles and PVA/glycerol.

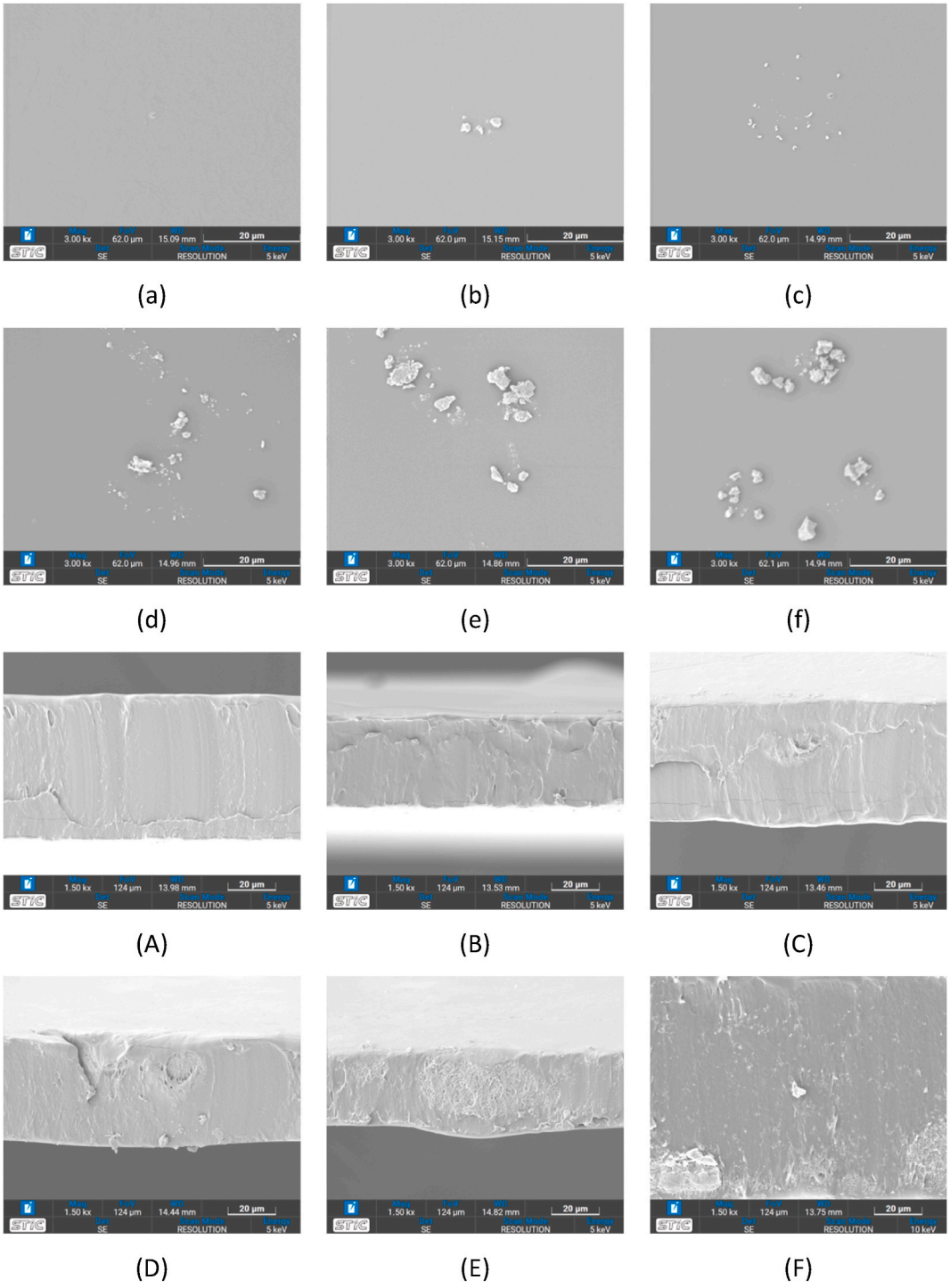

Fig. 4. SEM images of the surface and the cross-section of the composite films. The images correspond to different compositions: PVA-Si-0 (a) & (A); PVA-Si-0.5 (b) & (B); PVA-Si-1 (c) & (C); PVA-Si-3 (d) & (D); PVA-Si-5 (e & (E); PVA-Si-7 (f) & (F), respectively.

3.5. Mechanical properties

The mechanical properties of all composite films are presented in Fig. 5. While the EAB of films declined dramatically (Fig. 5a), the TS of PVA films first climbed and subsequently significantly decreased with an increase in Silica content (above 3%). When compared to pure PVA film, the TS of the film containing 1% silica reached a maximum point and rose by over 50 % (Fig. 5b). This finding

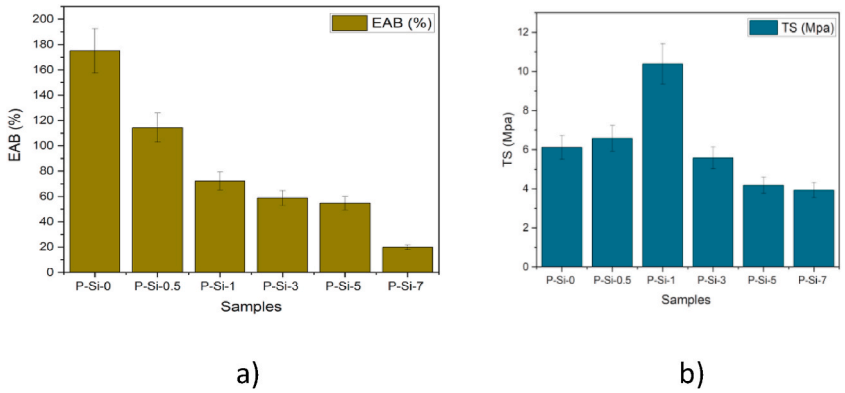

Fig. 5. Mechanical analysis EAB(a) and TS(b) for PVA-Si composites films.

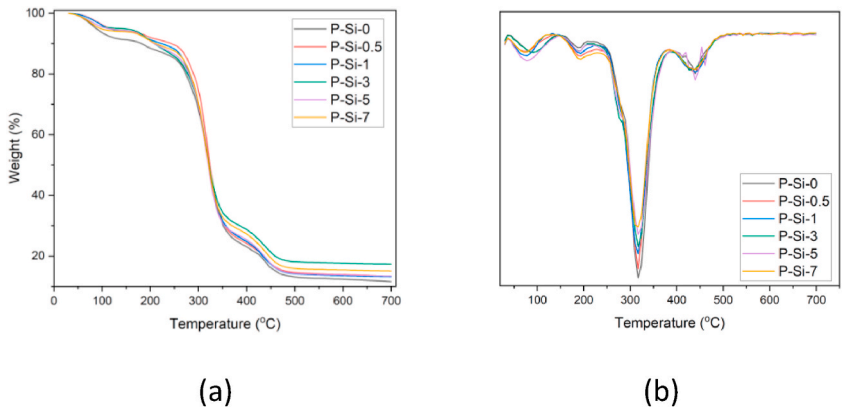

Fig. 6. TGA curves of the PVA/Si composites film.

suggests that PVA and Silica combine to produce significant interfacial contact and efficient stress transmission. It could be due to efficient hydrogen bonding interactions between Silica and carbonyl groups of PVA.

As a consequence, the films' flexibility was decreased, and their mechanical strength was enhanced. The TS was reduced for PVA composite film mixed with 3, 5, and 7 wt% silica than for PVA/Glycerol film without silica. When the percentage of Silica exceeded 1 wt%, it showed that the effects of TS were of lower quality. It may be because of the forming agglomerations when higher silica concentration, leading to the production of stress concentration spots when stretching. It would impair the functionality of the film's physical structure.

This was consistent with other outcomes obtained by adding solid additives to the polymer matrix, such as nano-SiO_2 and montmorillonite [1]. The starch/PVA films with 2.5% nano-SiO_2 added had the highest TS of all the films when the concentration of nano-SiO_2 was increased from 0% to 5% [44], whereas the blend films' EAB slowly dropped [45].

3.6. Thermal characterization

Fig. 6 displayed the TGA thermographs and derivative thermogravimetric (DTG) curves for each film. All PVA films degraded thermally in three stages, as demonstrated in Fig. 6a. The first weight loss was observed from 40 °C to 260 °C, which is when water begins to evaporate. Due to PVA's chain disintegration, a second weight loss occurred between 280 °C and 330 °C. The last stage is the decomposition of the PVA main chain and following degradation into carbon char at a range of 340 °C to 500 °C. As shown in Fig. 6b, the decomposition temperature of the PVA-Silica composite films is higher than that of pure PVA film. Additionally, when the amount of silica increased, the temperature of breakdown increased slightly. It showed that the films' thermal stability had improved as a result of the silica addition. Due to silica's effective heat insulation and gas barrier capabilities, the chain transfer process and the passage of volatile breakdown products through materials are both limited [37]. Which these properties, the biodegradable composite film is made from PVA (Polyvinyl Alcohol), silica, and glycerol which can have various practical applications due to its unique properties. This composite film can offer a combination of flexibility, mechanical strength, and barrier properties, for example - biodegradable mulch films, which can be used in agriculture as biodegradable mulch films to reduce weed growth and maintain soil moisture. It can be left in the field, gradually breaking down without harming the environment. Secondly, PVA-silica-glycerol films can be used for solar control applications to reduce heat and UV radiation transmission through windows. This composite film also can be used in

wrapping applications [46].

4. Conclusion

Silica nanoparticles, extracted from BA-MSWI, with a purity of 82.56%, were employed as reinforcement in plasticized polyvinyl alcohol (PVA) films containing glycerol. The addition of silica in varying weight percentages (0.5, 1, 3, 5, and 7 wt%) resulted in notable enhancements in the mechanical and thermal stability of the composite wrapping films. As expected, the presence of silica increased and led to a slight rise in the temperature of degradation. Remarkably, the incorporation of 1 wt% silica in the films resulted in a significant improvement in tensile strength, with a 50% increase compared to silica-free samples. Conversely, the introduction of silica resulted in reduced flexibility of the wrapping films. In summary, PVA-glycerol composite films loaded with 1% silica exhibited the best performance for biodegradable wrapping applications, providing a slightly transparent appearance, enhanced tensile strength, and a sufficient level of flexibility (approximately 120%) for wrapping purposes.

CRediT authorship contribution statement

Phan Thi Hong Hanh: Conceptualization, Data curation, Formal analysis, Investigation, Methodology, Validation, Writing – original draft. **Thitipone Suwunwong:** Conceptualization, Data curation, Formal analysis, Investigation, Methodology, Resources, Validation, Visualization, Writing – review & editing. **Suchada Chantrapromma:** Data curation, Methodology, Resources, Validation, Visualization, Writing – review & editing. **Patcharanan Choto:** Investigation, Methodology, Resources, Validation, Visualization, Writing – review & editing. **Chuleeporn Thanomsilp:** Data curation, Formal analysis, Investigation, Methodology, Resources, Writing – review & editing. **Khamphe Phoungthong:** Conceptualization, Funding acquisition, Methodology, Project administration, Resources, Supervision, Validation, Writing – review & editing.

Declaration of competing interest

The authors declare that they have no known competing financial interests or personal relationships that could have appeared to influence the work reported in this paper.

Acknowledgement

This research was supported by National Science, Research and Innovation Fund (NSRF), and Prince of Songkla University (Grant No. ENV6505018S). Received funding to support activities promoting research and innovation from Hub of Waste Management for Sustainable Development by HSM and the National Research Council of Thailand (NRCT). We would like to acknowledge Mae Fah Luang University for this study and carrying out this research.

Appendix A. Supplementary data

Supplementary data to this article can be found online at https://doi.org/10.1016/j.heliyon.2024.e25963.

References

[1] M. Batra, G.K. Malik, J. Mitra, Enhancing the properties of gelatin–chitosan bionanocomposite films by incorporation of silica nanoparticles, J. Food Process. Eng. 43 (2) (2020) 1–12, https://doi.org/10.1111/jfpe.13329.
[2] J. Jacob, V. Robert, R.B. Valapa, S. Kuriakose, S. Thomas, S. Loganathan, Poly(lactic acid)/Polyethylenimine Functionalized mesoporous silica Biocomposite films for food packaging, ACS Appl. Polym. Mater. 4 (7) (2022) 4632–4642, https://doi.org/10.1021/acsapm.1c01551.
[3] Z. Yu, B. Li, J. Chu, P. Zhang, Silica in situ enhanced PVA/chitosan biodegradable films for food packages, Carbohydr. Polym. (2017), https://doi.org/10.1016/j.carbpol.2017.12.043.
[4] N. Limpan, T. Prodpran, S. Benjakul, S. Prasarpran, Influences of degree of hydrolysis and molecular weight of poly(vinyl alcohol) (PVA) on properties of fish myofibrillar protein/PVA blend films, Food Hydrocolloids 29 (1) (2012) 226–233, https://doi.org/10.1016/j.foodhyd.2012.03.007.
[5] A.M. Youssef, Polymer nanocomposites as a New Trend for packaging applications, Polym. Plast. Technol. Eng. 52 (7) (2013) 635–660, https://doi.org/10.1080/03602559.2012.762673.
[6] M.Ö. Alaş, G. Doğan, M.S. Yalcin, S. Ozdemir, R. Genç, Multicolor Emitting carbon Dot-Reinforced PVA composites as edible food packaging films and Coatings with antimicrobial and UV-blocking properties, ACS Omega 7 (34) (2022) 29967–29983, https://doi.org/10.1021/acsomega.2c02984.
[7] F. Films, et al., Preparation and performance of radiata-pine-derived polyvinyl alcohol/carbon quantum dots fluorescent films, Materials 13 (1) (2020) 67.
[8] W. Yang, G. Qi, J.M. Kenny, D. Puglia, P. Ma, Effect of cellulose nanocrystals and lignin nanoparticles on mechanical, antioxidant and water vapour barrier properties of glutaraldehyde crosslinked PVA films, Polymers 12 (6) (2020), https://doi.org/10.3390/POLYM12061364.
[9] S.C. George, G. Groeninckx, K.N. Ninan, S. Thomas, Molecular Transport of Aromatic Hydrocarbons through Nylon-6/Ethylene Propylene Rubber Blends : Relationship, 2000, pp. 2136–2153.
[10] J. Seo, J. Jeon, Y.G. Shul, H. Han, Water sorption and activation energy in polyimide thin films, J. Polym. Sci., Part B: Polym. Phys. 38 (21) (2000) 2714–2720, https://doi.org/10.1002/1099-0488(20001101)38, 21<2714::AID-POLB20>3.0.CO;2-6.
[11] A. Shimazu, T. Miyazaki, T. Matsushita, M. Maeda, K. Ikeda, Relationships between chemical structures and solubility, diffusivity, and permselectivity of 1,3-butadiene and n-butane in 6FDA-based polyimides, J. Polym. Sci., Part B: Polym. Phys. 37 (21) (1999) 2941–2949, https://doi.org/10.1002/(SICI)1099-0488(19991101)37, 21<2941::AID-POLB4>3.0.CO;2-5.
[12] W.H. Lin, R.H. Vora, T.S. Chung, Gas transport properties of 6FDA-durene/pPDA copolyimides, J. Polym. Sci., Part B: Polym. Phys. 38 (2000) 2703.

[13] N. Artzi, A. Tzur, M. Narkis, A. Siegmann, The effect of extrusion processing conditions on EVOH/clay nanocomposites at low organo-clay contents, Polym. Compos. 26 (3) (2005) 343–351, https://doi.org/10.1002/pc.20096.

[14] N. Artzi, M. Narkis, A. Siegmann, Review of melt-processed nanocomposites based on EVOH/organoclay, J. Polym. Sci., Part B: Polym. Phys. 43 (15) (2005) 1931–1943, https://doi.org/10.1002/polb.20481.

[15] H. Kjellgren, M. Gällstedt, G. Engström, L. Järnström, Barrier and surface properties of chitosan-coated greaseproof paper, Carbohydr. Polym. 65 (4) (2006) 453–460, https://doi.org/10.1016/j.carbpol.2006.02.005.

[16] D. Kim, S.W. Kim, Barrier property and Morphology of Polypropylene/Polyamide blend film, Kor. J. Chem. Eng. 20 (4) (2003) 776–782, https://doi.org/10.1007/BF02706923.

[17] Y. Liu, Y. Liu, S. Wei, Processing technologies of EVOH/nano-SiO_2 high-barrier packaging composites," 17th IAPRI World, Conf. Packag. 2010 (2010) 269–274.

[18] N.M. Barkoula, B. Alcock, N.O. Cabrera, T. Peijs, Flame-retardancy properties of Intumescent Ammonium poly(Phosphate) and Mineral Filler Magnesium hydroxide in combination with Graphene, Polym. Polym. Compos. 16 (2) (2008) 101–113, https://doi.org/10.1002/pc.

[19] Z. Yang, H. Peng, W. Wang, T. Liu, Crystallization behavior of poly(ε-caprolactone)/layered double hydroxide nanocomposites, J. Appl. Polym. Sci. 116 (5) (2010) 2658–2667, https://doi.org/10.1002/app.

[20] N.A. Al-tayyar, A.M. Youssef, R.R. Al-hindi, Antimicrobial packaging e ffi ciency of ZnO-SiO 2 nanocomposites infused into PVA/CS fi lm for enhancing the shelf life of food products, Food Packag. Shelf Life 25 (2020) 100523, https://doi.org/10.1016/j.fpsl.2020.100523.

[21] M.S. Sarwar, M.B.K. Niazi, Z. Jahan, T. Ahmad, A. Hussain, Preparation and characterization of PVA/nanocellulose/Ag nanocomposite films for antimicrobial food packaging, Carbohydr. Polym. 184 (January) (2018) 453–464, https://doi.org/10.1016/j.carbpol.2017.12.068.

[22] Z.W. Abdullah, Y. Dong, Biodegradable and water resistant poly(vinyl) alcohol (PVA)/starch (ST)/glycerol (GL)/halloysite nanotube (HNT) nanocomposite films for sustainable food packaging, Front. Mater. 6 (April) (2019) 1–17, https://doi.org/10.3389/fmats.2019.00058.

[23] B.R. Moreira, M.A. Pereira-Júnior, K.F. Fernandes, K.A. Batista, An ecofriendly edible coating using cashew gum polysaccharide and polyvinyl alcohol, Food Biosci. 37 (2020), https://doi.org/10.1016/j.fbio.2020.100722.

[24] A.M. Mebert, C.J. Baglole, M.F. Desimone, D. Maysinger, Nanoengineered silica: properties, applications and toxicity, Food Chem. Toxicol. 109 (2017) 753–770, https://doi.org/10.1016/j.fct.2017.05.054.

[25] F. Bi, X. Zhang, J. Liu, H. Yong, L. Gao, J. Liu, Development of antioxidant and antimicrobial packaging fi lms based on chitosan , D- α -tocopheryl polyethylene glycol 1000 succinate and silicon dioxide nanoparticles, Food Packag. Shelf Life 24 (2020) 100503, https://doi.org/10.1016/j.fpsl.2020.100503 no. December 2019.

[26] R. Zhang, X. Wang, M. Cheng, Preparation and Characterization of Potato Starch, 2018, pp. 9–12, https://doi.org/10.3390/polym10101172.

[27] G.C.C. Yang, T.Y. Yang, Synthesis of zeolites from municipal incinerator fly ash, J. Hazard Mater. 62 (1) (1998) 75–89, https://doi.org/10.1016/S0304-3894(98)00163-0.

[28] Y. Fan, F.S. Zhang, J. Zhu, Z. Liu, Effective utilization of waste ash from MSW and coal co-combustion power plant-Zeolite synthesis, J. Hazard Mater. 153 (1–2) (2008) 382–388, https://doi.org/10.1016/j.jhazmat.2007.08.061.

[29] G. Chandrasekar, K.S. You, J.W. Ahn, W.S. Ahn, Synthesis of hexagonal and cubic mesoporous silica using power plant bottom ash, Microporous Mesoporous Mater. 111 (1–3) (2008) 455–462, https://doi.org/10.1016/j.micromeso.2007.08.019.

[30] D. Chen, et al., Municipal solid waste incineration residues recycled for typical construction materials—a review, RSC Adv. 12 (10) (2022) 6279–6291, https://doi.org/10.1039/d1ra08050d.

[31] Z.S. Liu, W.K. Li, C.Y. Huang, Synthesis of mesoporous silica materials from municipal solid waste incinerator bottom ash, Waste Manag. 34 (5) (2014) 893–900, https://doi.org/10.1016/j.wasman.2014.02.016.

[32] N.U. Amin, S. Khattak, S. Noor, I. Ferroze, Synthesis and characterization of silica from bottom ash of sugar industry, J. Clean. Prod. 117 (2016) 207–211, https://doi.org/10.1016/j.jclepro.2016.01.042.

[33] B. Ruiz, R.P. Girón, I. Suárez-Ruiz, E. Fuente, From fly ash of forest biomass combustion (FBC) to micro-mesoporous silica adsorbent materials, Process Saf. Environ. Protect. 105 (2017) 164–174, https://doi.org/10.1016/j.psep.2016.11.005.

[34] C.V.L. Giosafatto, A. Al-Asmar, A. D'Angelo, V. Roviello, M. Esposito, L. Mariniello, Preparation and characterization of bioplastics from grass pea flour cast in the presence of microbial transglutaminase, Coatings 8 (12) (2018), https://doi.org/10.3390/coatings8120435.

[35] M. Pereda, G. Amica, I. Rácz, N.E. Marcovich, Structure and properties of nanocomposite films based on sodium caseinate and nanocellulose fibers, J. Food Eng. 103 (1) (2011) 76–83, https://doi.org/10.1016/j.jfoodeng.2010.10.001.

[36] T.A. Nascimento, V. Calado, C.W.P. Carvalho, Development and characterization of flexible film based on starch and passion fruit mesocarp flour with nanoparticles, Food Res. Int. 49 (1) (2012) 588–595, https://doi.org/10.1016/j.foodres.2012.07.051.

[37] N. Pacheco, et al., Effect of bio-chemical chitosan and gallic acid into rheology and physicochemical properties of ternary edible films, Int. J. Biol. Macromol. 125 (2019) 149–158, https://doi.org/10.1016/j.ijbiomac.2018.12.060.

[38] H. Tian, D. Liu, Y. Yao, S. Ma, X. Zhang, A. Xiang, Effect of Sorbitol plasticizer on the structure and properties of melt processed polyvinyl alcohol films, J. Food Sci. 82 (12) (2017) 2926–2932, https://doi.org/10.1111/1750-3841.13950.

[39] E.S. Costa-Júnior, E.F. Barbosa-Stancioli, A.A.P. Mansur, W.L. Vasconcelos, H.S. Mansur, Preparation and characterization of chitosan/poly(vinyl alcohol) chemically crosslinked blends for biomedical applications, Carbohydr. Polym. 76 (3) (2009) 472–481, https://doi.org/10.1016/j.carbpol.2008.11.015.

[40] B. Shokri, M.A. Firouzjah, S.I. Hosseini, FTIR analysis of silicon dioxide thin film deposited by metal organic-based PECVD, Proc. 19th Int. Plasma Chem. Soc. (2009) 1–4. www.ispc-conference.org.

[41] S.A. Pirzada, Tahira, Sara A. Arvidson, Carl D. Saquing, S. Sakhawat Shah, Khan, Hybrid Silica−PVA Nanofibers via Sol−Gel Electrospinning, pdf, 2012, pp. 5834–5844.

[42] S. Tripathi, G.K. Mehrotra, P.K. Dutta, Preparation and physicochemical evaluation of chitosan/poly(vinyl alcohol)/pectin ternary film for food-packaging applications, Carbohydr. Polym. 79 (3) (2010) 711–716, https://doi.org/10.1016/j.carbpol.2009.09.029.

[43] M. Yang, J. Shi, Y. Xia, Effect of SiO_2, PVA and glycerol concentrations on chemical and mechanical properties of alginate-based films, Int. J. Biol. Macromol. 107 (2018) 2686–2694, https://doi.org/10.1016/j.ijbiomac.2017.10.162.

[44] C. Chen, et al., Effects of montmorillonite on the properties of cross-linked poly(vinyl alcohol)/boric acid films, Prog. Org. Coating 112 (2017) 66–74, https://doi.org/10.1016/j.porgcoat.2017.06.003.

[45] S. Tang, P. Zou, H. Xiong, H. Tang, Effect of nano-SiO_2 on the performance of starch/polyvinyl alcohol blend films, Carbohydr. Polym. 72 (3) (2008) 521–526, https://doi.org/10.1016/j.carbpol.2007.09.019.

[46] M. R, K.M. Suhasini, S. Rajeshwari, A.B. Bindya, P.M. Hemavathi, A. Vishwanath, R. Syed, R.G. Eswaramoorthy, C. Amachawadi, V. Shivamallu, K. Chattu, S. S. Majani, Pectin/PVA and pectin-MgO/PVA films: Preparation, characterization and biodegradation studies, Heliyon 9 (5) (2023), https://doi.org/10.1016/j.heliyon.2023.e15792.